MASTER

# SIMULATION OF LMFBR EXCURSION MODELS BY MEANS OF ICECO

CONF-770807--52

A. H. Marchertas, Y. C. Wang, S. H. Fistedis

Prepared for

4th SMIRT Conference
San Francisco, CA
August 15-19, 1977



ARGONNE NATIONAL LABORATORY, ARGONNE, ILLINOIS

UofC-AUA-USERDA

operated under contract W-31-109-Eng-38 for the
U. S. ENERGY RESEARCH AND DEVELOPMENT ADMINISTRATION

## 1. Introduction

A comparison was presented in a recent paper [1] between the data derived from simple LMFBR containment models and the predictions of ANL codes adaptable for such an analysis. The test data used were taken from a series of experiments dealing with the simulation studies of the SNR-300 reactor. Since that comparison was made, additional experimental data has become available in a Belgonucleaire report by Egléme et al. [2], which are again compared with the ANL containment code solutions.

The previous paper [1] provided comparisons between experimental data and analytical solutions by two ANL codes: REXCO [3] and ICECO [4,5]. Thus, the material presented there dealt with solutions which could be equally obtained by both codes. In this paper we are more concerned with purely simulating the tests and do utilize the codes which fit the requirement of the problem.

The added feature of fluid spillage, which is a subject of some concern in experiments, is modeled in the ICECO code and will be stressed here. Several variations of spillage solution were arrived at gaining more insight to this problem and thus serve in reducing some of the uncertainties connected with fluid spillage. Other additional features of the analytical models, which were not available in the previous presentation, are utilized and described in this paper.

## 2. The Test Models

An extensive test program was conducted to simulate the SNR-300 hypothetical core disruptive accident (HCDA) in scaled models [8]. To this end, simplified axisymmetric models involving different radial boundary constraints, a number of fluid surface levels, and models with other parametric variations were tested. Computer codes were also applied aimed at correlating the measured test data. Such correlations resulted in a corresponding pressure-volume description of the applied source.

Three test configurations of the SNR-300 reactor models shown in fig. 1 will be considered in this paper. The first two models differ only by the rigidity of their radial boundary and the description of the source. The third model is essentially the same as that in fig. 1b, except that two cylindrical vessels exist. In all cases, the basic test configuration consists of a spherical pressure-volume source immersed within a pool of water, which in turn, is held by a cylindrical container with rigid ends. From the free surface of the water to the top of the container, the space is occupied by air. The cylindrical walls of the containers are pre-compressed by the rigid end plates with holddown bolts. Rubber seals separate the cylindrical walls from the end plates.

The pressure-volume relationships of the source are derived independently and are given in Tables I and II. The dynamic response of the structural material is also separately established by appropriate dynamic tests.

## 3. Analytical Models and Comparison with Test Data

The bottom boundary of the tank in all the analytical models is assumed to be rigid and fixed in space. The top cover boundary, when fluid spillage is taken into consideration, is assumed to be rigid but can be displaced vertically, the constraint of this motion being the mass of the cover and the rigidity (stretching) of the holddown bolts. It should be noted that in the experiment the holddown bolts prestress the cylindrical wall through the rigid end plates; the end plates separate the cylinder of rubber seals. Thus, an exact analytical representation of the boundary conditions of the test vessel is beyond the capability of the codes. However, taking into consideration the description of the test, led us to modeling these boundary conditions in the following manner: (a) the bottom boundary was assumed to be constrained axially, but was free to move radially, and (b) the top boundary was assumed to be completely free of any constraints.

The equation of state of water used in these analytical models was the so-called Tait formulation

$$p = 3.047\ (\rho^{7.15}-1) \tag{1}$$

where p is the pressure in bars and $\rho$ is the density. The air equation of state was taken to be

$$p = (V_o/V)^{1.3} \tag{2}$$

where p is in kb, V is the volume, and $V_o$ is the initial volume.

### 3.1 Thick Vessel Model

The analytical ICECO model of this configuration shown in fig. 1a assumes that the vessel deforms elastically; the pressure-volume input of the source is given in Table I.

Although experimental-analytical comparisons pertaining to configurations shown in Fig.1a were presented in ref. [1], one additional point is brought out in this paper. This point deals with the actual displacement of the top lid, and has to do with the spillage model incorporated within ICECO.

The experimental data of three holddown bolts is taken from ref. [2] and are reproduced in fig. 2. The first pressure peak is interpreted as the response of the bottom of the tank due to the initial pressure pulse. After this effect has subsided, the second sharp stress is recorded, which should be due to the effect of slug impact. It should be noted that the two major stress peaks are sufficiently far apart in time that their interplay may be decoupled and the two could be treated separately.

The results of the ICECO spillage model provide the movement of the top cover during slug impact. Because of the rigid-body assumption for the top cover, this displacement can be related to the elongation of the bolts if elastic behavior is assumed. Thus, after converting the displacement to stress by using the bolt length of 1.23 m and the elastic modulus of $2 \times 10^4$ kp/mm$^2$, the results were superimposed in fig. 2 over the experimental bolt stresses taken from ref. [2]. The time scale of the analytical results was changed to correspond to the second peak of the experimental data.

### 3.2 Thin Vessel Configuration

The assumptions made in the ICECO model are similar to those for the thick-elastic-vessel configuration, except that the thin vessel is permitted to deform plastically. The stress-strain curve assumed for the thin vessel is confined to a bilinear representation. The elastic portion with modulus E = 20000 kp/mm$^2$ extends to the stress of 44 kp/mm$^2$; beyond the yield stress, a plastic modulus $E_p$ = 40.96 kp/mm$^2$ is assumed.

The pressure-volume source characteristics used with the model shown in fig. 1b are taken from ref. [7] and given in Table II.

In the original solution of the thin vessel problem it was assumed that air occupies the space between the surface of the water and the bottom of the cover, and spillage of the fluid does not take place. [1] This solution is reproduced in fig. 3, showing in sequence the configurations: (a) the initial grid of the analytical model, (b) the configuration at about the maximum vessel deformation, opposite the source, (c) the initiation of impact, and (d) the maximum deformed configuration at the top of the vessel. It is clearly observed that during the initial stage of vessel deformation at the bottom and opposite the source, it deforms not only in the radial direction but also axially. The axial deformation of the vessel at the top is of the order of about 25 mm before the slug impact. Making an allowance for the contraction of the bolts during the initial deformation of the vessel, which would be a small fraction of one centimeter, we can see an initial opening on the top before impact takes place. The effectiveness of the rubber seals in a case like this should be negligible. Therefore, spillage of fluid for the thin vessel model could be considerable and the displacement at the top of the vessel may be quite different than what is shown in fig.3.

The uncertainity of water spillage through the existing gap at the top of the vessel on the deformation of the vessel led to two additional runs of ICECO. One run enabled fluid spillage over the top of the vessel during slug impact. Since the Eulerian grid was stationary and the vessel top moved within the grid, some initial matching of grid size was made so that spillage would approximately be through at least one full grid dimension. The axial grid size was chosen as exactly half of that of the previous model. Consequently, the difference of this run was that the axial grid size was doubled, and air plus water was free to flow radially through the top-most grid during and after the slug impact. The progression of slug impact, fluid spillage and vessel deformation at the top is shown in figs. 4a through 4d. It may be observed that the top of the vessel now deforms less than in the previous solution shown in fig. 3. In fact, while the top of the vessel without spillage and air above the water surface was about 17.5%, the permanent set with spillage and no air on the top was found to be about 12%.

As a still different variations dealing with slug impact and a consequent vessel deformation at the top, another ICECO run was made assuming that no air existed at the top of the water surface, but spillage of the fluid was not considered. This variation thus only eliminated the air from the first solution depicted in fig. 3. The resultant vessel deformation of this run was found to be between those derived from the first two solutions. The final vessel deformations of all three analytical solutions are shown in fig. 5, together with the experimental results presented in ref. [2].

### 3.3 Double-Vessel Model

The combination of two codes REXCO and ICECO is utilized in this problem to yield the final analytical deformation of the cylindrical vessels. This is necessary because of basic or current limitations of the individual codes. The complexity revolves around the double-connected regions of water, spillage and even mixing of both domains. The REXCO code, which is based on Lagrangian formulation, is handicapped by large deformations which would be a part of spillage over the top of inner vessel during slug impact. The ICECO code at this point of development does not treat an internal thin vessel. Thus, the analytical modeling of the two-vessel problem is decomposed into two parts: the first part involves the REXCO code and provides the initial solution to the problem. The second part makes use of the ICECO code and continues the solution to the end. The source characteristics for both models are the same as for the thin-vessel model discussed before. A bilinear behavior of the vessel is assumed; an elastic portion with $E = 2 \times 10^4$ kp/mm$^2$ extends to a yield stress of 39.2 kp/mm$^2$ after which a plastic modulus of 37.3 kp/mm$^2$ is assumed.

The initial stage of the excursion by means of REXCO is extended to the time when the vessels at the bottom and opposite the source have deformed to their equilibrium. At this time (1.4 ms) the REXCO output is converted for input of ICECO. An averaging procedure is applied within the fluid to approximate the initial velocities, densities and pressures for the initial conditions of the ICECO solutions.

The ICECO solution commences with a single fluid domain, a simple vessel and simulates slug impact with the resultant fluid spillage. A special assumption made in the ICECO solution is that at the transition the vessel is taken to be undeformed. The lower part of this new vessel extending to 620 mm is now assumed very thick (50 mm). Above this point, the vessel retains its actual thickness. The reasons for specifying a rigid vessel portion at the bottom is because at 1.4 ms, the vessel had deformed permanently and further deformation would not be expected; the thick-vessel portion would confine the deformations to small elastic oscillations which should not be detrimental to the overall solution. The actual thickness of the vessel at the top should enable permanent plastic deformation to take place during slug impact. The junction of the thin-thick portions is placed supposedly sufficiently far from the top so that the effective artificial reinforcement of the thick-vessel portion should be small. The final vessel deformations are thus derived from both REXCO and ICECO solutions are shown in fig. 6 also containing the experimental data for ref. [2].

The single vessel ICECO model thus provides the top deformation of the inner vessel. The top deformation of the outer vessel can not as yet be generated.

## 4. Concluding Remarks

The experimental data of bolt stresses as given in ref. [2] and reproduced in fig. 2 agree quite well with the deduced analytical upper lid displacement. The analytical results overestimate the experimental data only very slightly. The duration of the gap opening (which here corresponds to the stretching of the bolts) also checks quite well with the experimental data.

The thin vessel deformation yields also a fairly good check with two sets of experimental data as shown in fig. 5. As explained before, the discrepancy at the bottom is attributed to the inability of the code to match the test boundary conditions sufficiently well. The extent of vessel deformations at the top in all three analytical runs is also not as great as one may be initially led to believe. The differences are rather localized and decrease sharply with the distance from the top. It is significant that the case with no spillage and no air differs only slightly from the run with spillage. This indicates that the permanent vessel deformation is set rather early as compared to the rate of spillage; the effective pressure difference across the vessel is reduced only slightly by the amount of spilled fluid.

The permanent vessel deformations pertaining to the double-vessel configuration, as shown in fig. 6, exhibit also a fairly reasonable agreement between experiment and analysis. The rather large discrepancy at the bottom of the inside vessel is difficult to explain. One explanation for this deviation could be a possible separation of inner vessel from the bottom of the container during the initial stages of the excursion. Such a separation would enable fluid transfer across the bottom of the inner vessel thus reducing the pressure drop and in turn also the vessel deformation.

The deformation of the top of the inner vessel, as shown in fig. 6, is dependent on several

several assumptions made in the analysis. Some of them which relate to the combined REXCO-ICECO modeling can be mentioned. One of the implied assumptions made is that the vessel at the height separating the first phase of vessel deformation (bottom and opposite the source) with the second phase of deformation (due to slug impact) does not deform radially, or does so very little. In this connection the vessel of this ICECO model is composed of a thick and a thin wall position. The transition point of the thick-thin portions is the location which is initially assumed as non-deforming. The vessel deformation at the top must be affected by this transition point, unless it is located sufficiently far from that end. We have investigated the sensitivity of this transition point by making an additional ICECO run. Initially we had assumed the transition point to be at the height of 62 cm from the bottom; the resultant analytical deformation at the very top was obtained as 6%. The current data

The ICECO code, which provides most of the anlytical results described in this paper, is still in the process of continuous updating. Improvements are continuously being incorporated within the code with the intent of providing more options for the user. With this in mind, the ability of ICECO to treat multiple thin vessels should come in very soon. then the analysis of the double vessel will be possible without the need of combining codes, as was done here.

The treatment of the outer vessel at the instant of slug impact should also be possible in the near future. The special boundary condition for radial fluid impact would need to be added for this purpose. With this axial capability already available, the incorporation of radial boundary treatment should not be a major undertaking.

References


[1] MARCHERTAS, A. H., WANG, C. Y., and FISTEDIS, S. H., "A Comparison of ANL Containment Codes with Experiment," Int. Meeting on Fast Reactor Safety and Related Physics, Oct. 1976, Chicago.

[2] EGLÈME, M., et al., "NUCLEAR ACCIDENT Simulation Programme, Part III - Experiments in 1/13 scale vessels at JRC-Ispre (ITALY)," Topical Report BN 7510-01, Oct. 1975.

[3] CHANG, Y. W. and GVILDYS, J., "REXCO-HEP: A Two-Dimensional Code for Calculating the Primary System Response in Fast Reactors," Argonne National Laboratory Report ANL-75-19 (June 1975).

[4] WANG, CHUNG-YI, "ICECO - An Implicit Eulerian Method for Calculating Fluid Transients in Fast-Reactor Containment," Argonne National Laboratory Report, ANL-75-81 (Dec. 1975).

[5] WANG, CHUNG-YI, "An Implicit Eulerian Method for Analyzing Transient Phenomena in Fast Reactors," Proc. 12th Annual Meeting Soc. of Eng. Sci., U. of Texas, Austin (Cot. 1975), pp. 919-928.

[6] EGLÈME, M. et al., "Nuclear Accident Simulation Program, Part III - Experiments in 1/13th-Scale Vessels at J.R.C. - Ispra, Italy," Topical Report BN 7510-01, Brussels (October 1975).

[7] STIEVENART, M., et al., "Analysis of LMFBR Explosion Model Experiments by Means of the SURBOUM-II CODE," PaperE 3/5, 3rd Intl. Conf. on SMiRT, London, Sept. 1-5, 1975.

TABLE I

SOURCE CHARACTERISTICS FOR THE THICK-VESSEL MODEL* OF FIGURE 1a

| Pressure, bar | Volume Ratio ($V/V_o$) |
|---|---|
| 411 | 1 |
| 330 | 1.3 |
| 263 | 1.72 |
| 182 | 2.37 |
| 152 | 3.13 |
| 124 | 4.11 |
| 109 | 5.18 |
| 85 | 6.7 |
| 65.5 | 8.93 |
| 50 | 12 |
| 44 | 13.9 |
| 36 | 17.0 |
| 30.5 | 20.9 |
| 27 | 24.0 |
| 23.5 | 27.8 |
| 20 | 31.5 |
| 19.2 | 34.8 |

*These data are taken from Table III, ref. [7], and expanded by adding intermediate values obtained from a log-log plot.

TABLE II

SOURCE CHARACTERISTICS FOR THE THIN-AND DOUBLE VESSEL MODELS* OF FIGURES 1b & 1c

| Pressure, bar | Volume Ratio ($V/V_o$) |
|---|---|
| 426.8 | 1 |
| 380.8 | 1.18 |
| 278.9 | 1.60 |
| 199.3 | 2.12 |
| 111.7 | 2.75 |
| 71.4 | 3.47 |
| 42 | 5 |
| 22 | 8 |
| 12.2 | 12 |
| 7 | 18 |
| 3.8 | 28 |
| 1.95 | 45 |
| 1.1 | 68.5 |

*These data were taken from ref. [2] and expanded by adding intermediate values obtained from a log-log plot.

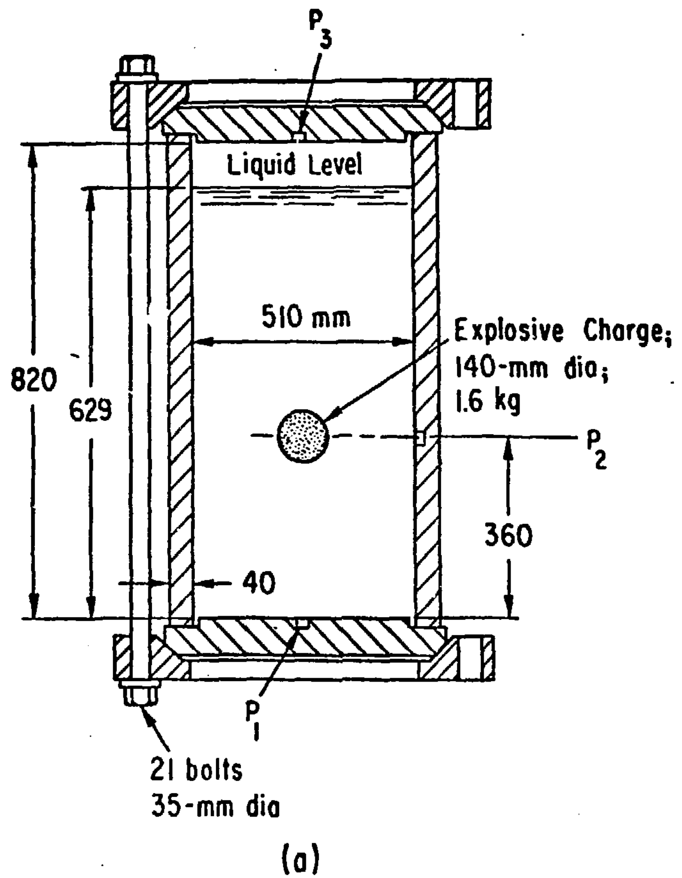


FIG. 1 TEST CONFIGURATIONS USED IN CONTAINMENT STUDIES

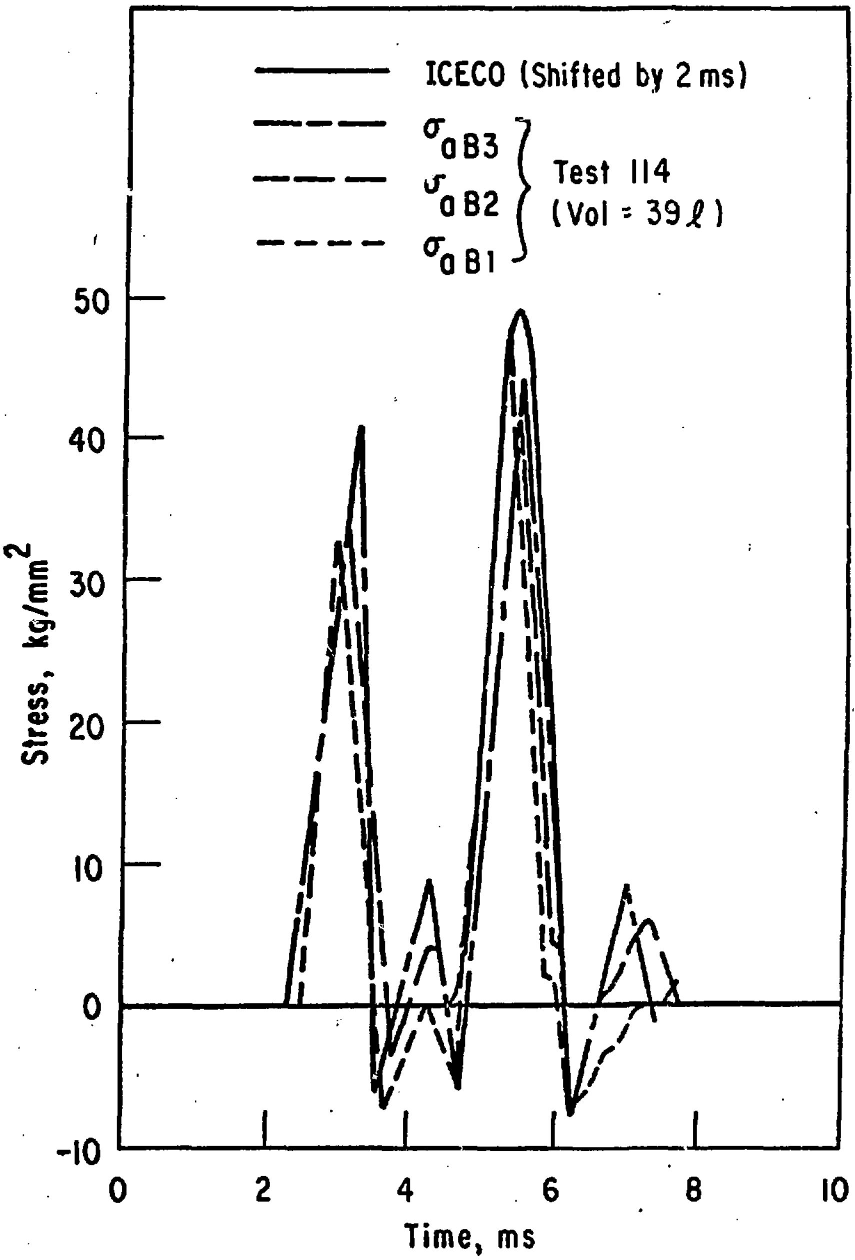


FIG. 2 HOLDDOWN BOLT RESPONSE COMPARISON

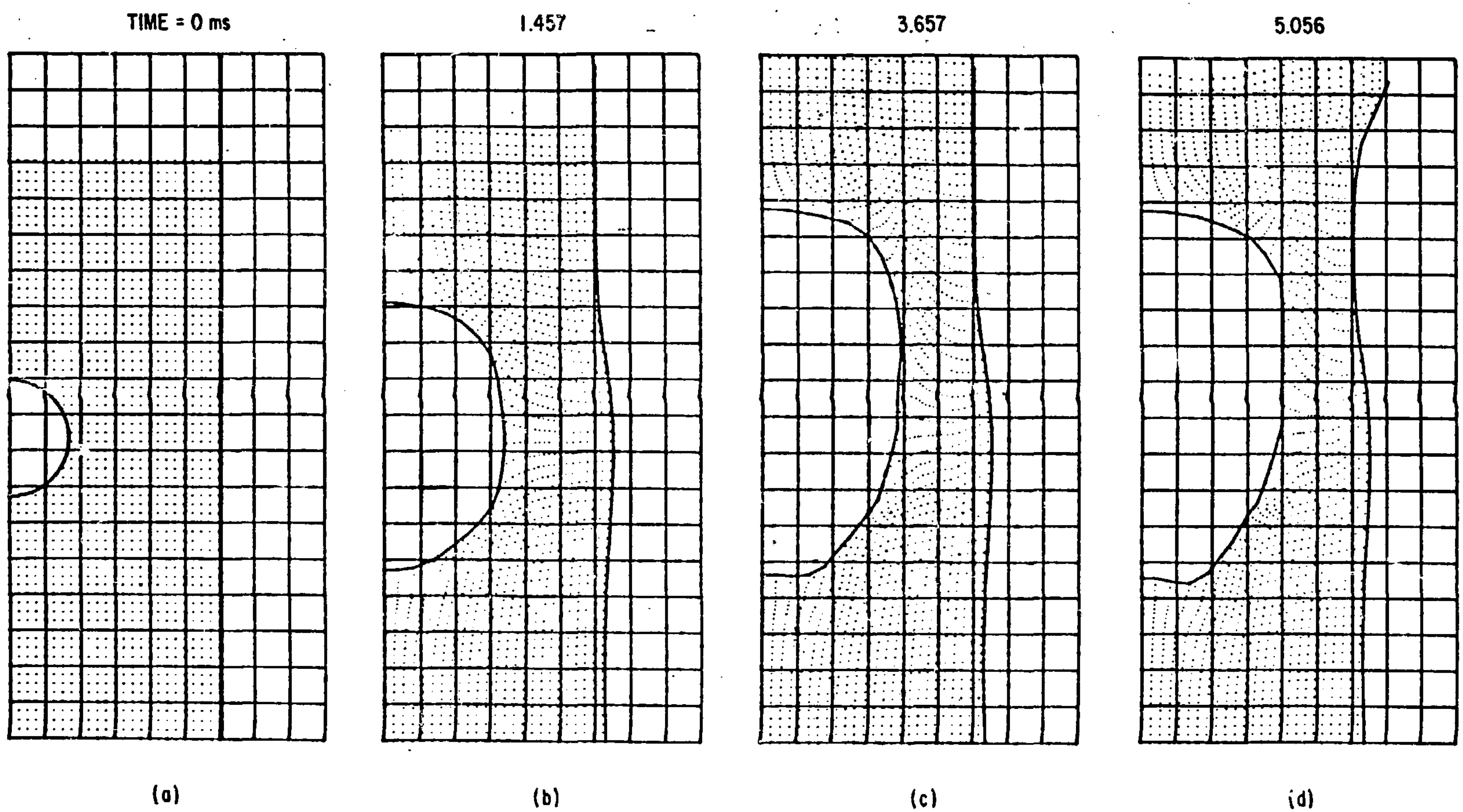


FIG. 3 THIN-VESSEL ~~[illegible]~~ RESULTS WITH AIR AND NO SPILLAGE

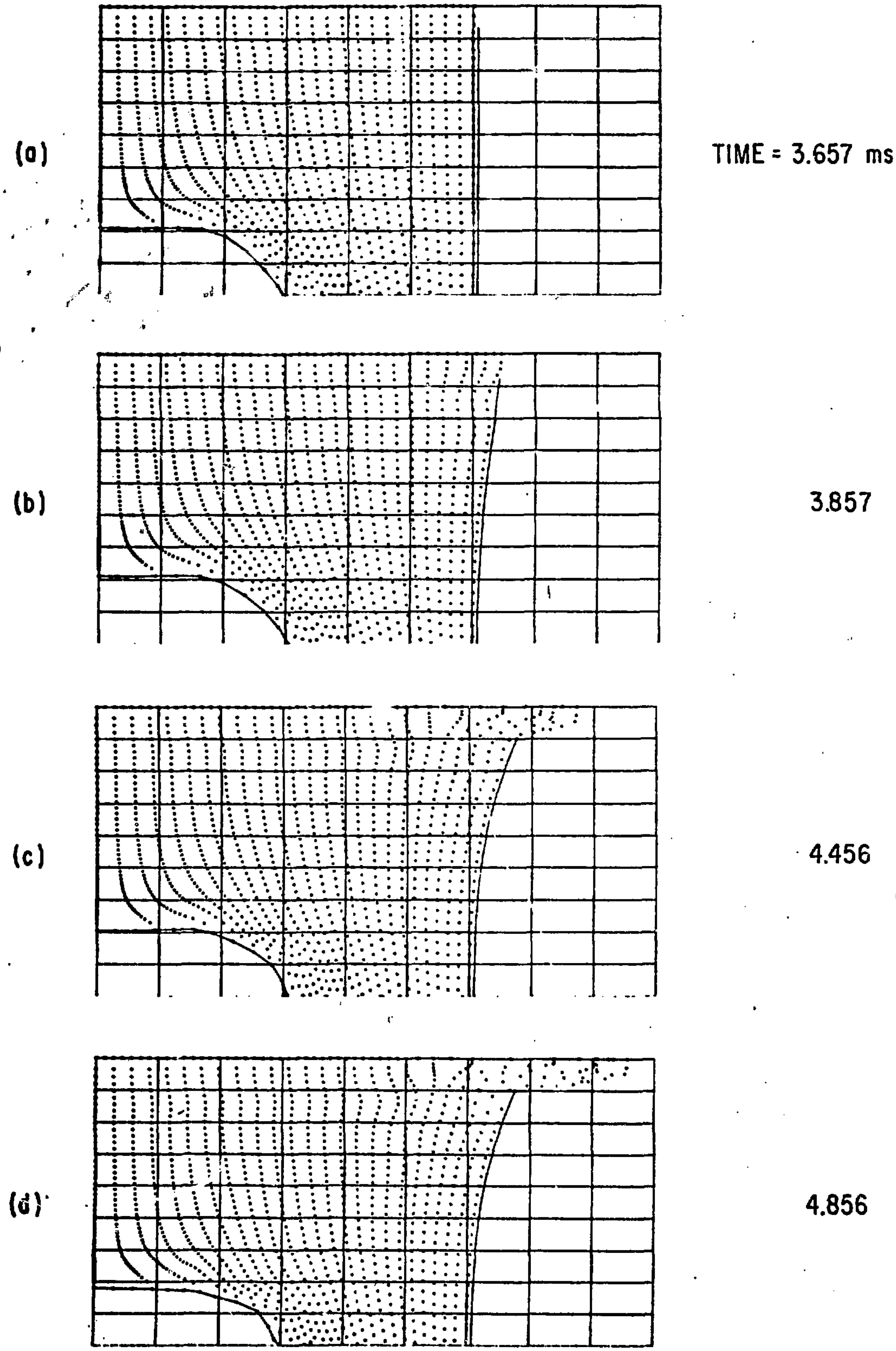


FIG. 4 SEQUENCE OF THIN-VESSEL RESULTS WITHOUT AIR AND WITH SPILLAGE

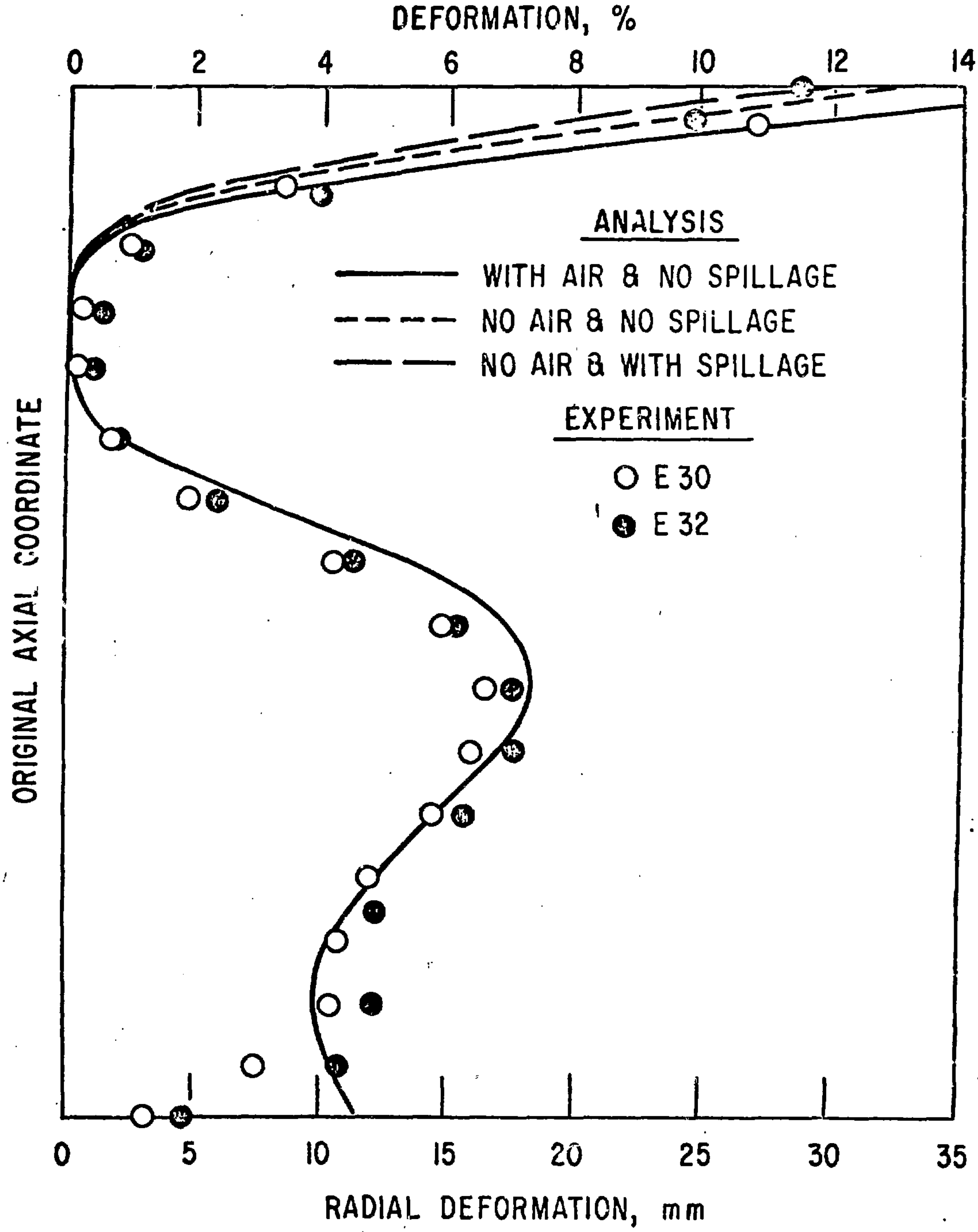


FIG. 5 COMPARISON OF PERMANENT THIN-VESSEL DEFORMATION

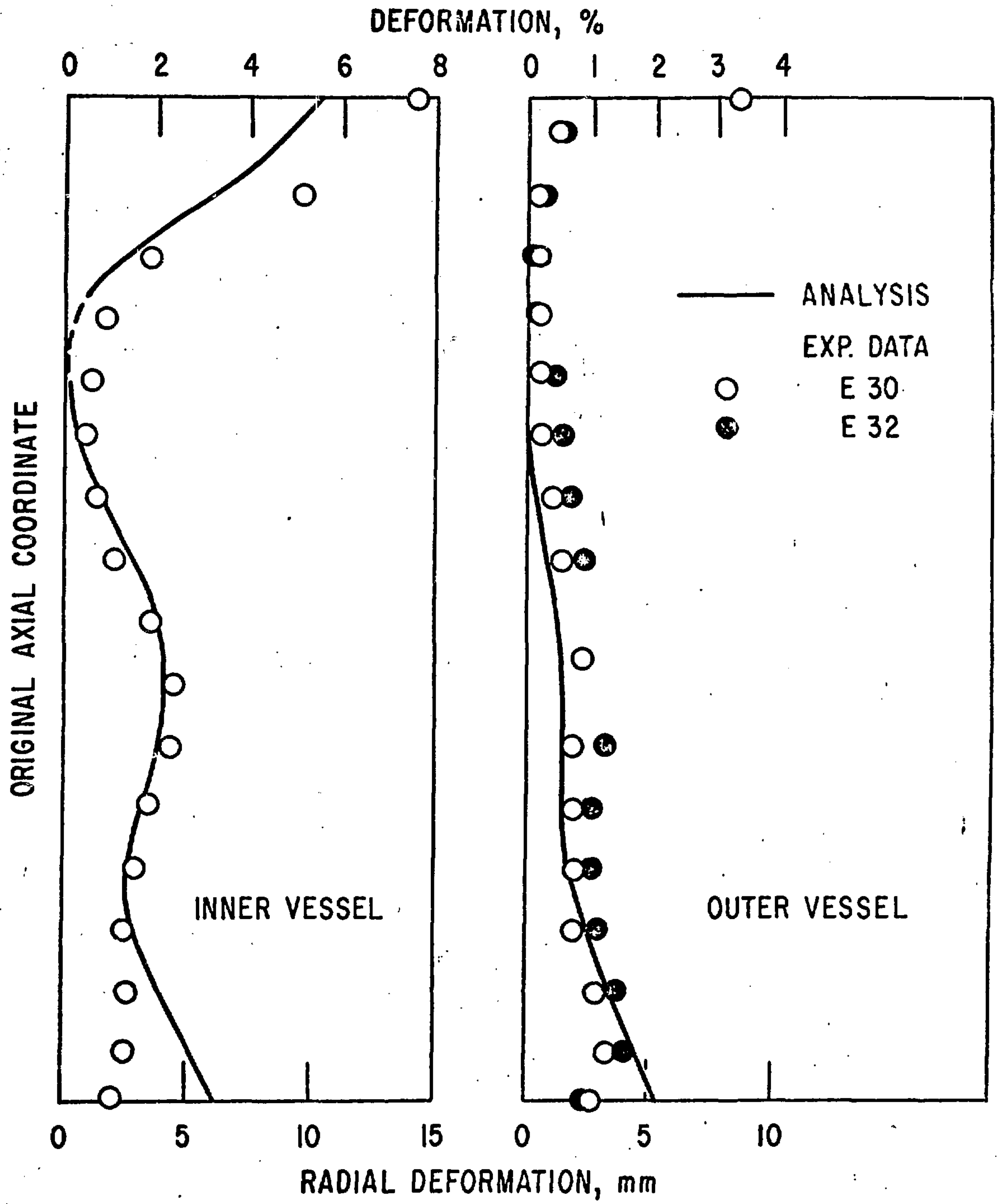


Fig. 6 Comparison of Double-Vessel Deformations